13th World Conference on Earthquake Engineering
Vancouver, B.C., Canada
August 1-6, 2004
Paper No. 2845

INCORPORATION OF REAL-TIME RECURRENCE PROBABILITIES, SITE RESPONSE EFFECTS, AND RUPTURE DIRECTIVITY EFFECTS IN SITE-SPECIFIC RESPONSE SPECTRA, UTAH STATE CAPITOL, SALT LAKE CITY, UTAH

Donald L. WELLS, Maurice S. POWER, Robert R. YOUNGS, and Shengzao CHEN[1]

SUMMARY

We performed probabilistic and deterministic seismic hazard analyses to develop site-specific horizontal and vertical response spectra for use in the seismic renovation program for the Utah State Capitol. We considered a range of earthquake source parameters, recurrence data, and Poissonian, real-time, and fault slip rate models to characterize the potential occurrence of large earthquakes on the nearby Wasatch fault. Both firm soil and soft rock attenuation relationships were used in the analysis. The rock results were modified for the firm soil site conditions using region-specific soil amplification factors. Near-field effects were incorporated from consideration of alternative rupture geometries.

INTRODUCTION

The Utah State Capitol Preservation Board has undertaken a comprehensive restoration and construction project for the purpose of renovating the Utah State Capitol in Salt Lake City, Utah. The purpose of this study was to develop site-specific response spectra of earthquake ground motions for use in the design of the seismic retrofit of the State Capitol building. The response spectra and other data presented in this paper are documented in detail in a report prepared by Geomatrix for AMEC Earth and Environmental, Inc. (AMEC [1]). These results were developed for use in evaluation and retrofit design of the Capitol consistent with guidelines of FEMA 356 (Federal Emergency Management Agency [FEMA] [2]).

The State Capitol was constructed between 1913 and 1915, is about 404 feet long (east-west) by 240 feet wide (north-south), and is 283 feet in height. The structural system includes a reinforced concrete frame and floor slabs, with granite and marble columns, and steel trusses in the roof and dome. The foundation consists of reinforced concrete spread footings (Cooper/Roberts Team [3]). The planned retrofit includes installation of a base isolation system at the level of the existing footings.

Geomatrix worked closely with personnel from AMEC Earth & Environmental, Inc. (Anaheim and Salt Lake City offices) in developing the response spectra, and with personnel at Reaveley Engineers, Salt

[1] Geomatrix Consultants, Inc., 2101 Webster Street, 12th Floor, Oakland, CA 94612, (510) 663-4100, (510) 663-4141, dwells@geomatrix.com; mpower@geomatrix.com; byoungs@geomatrix.com; schen@geomatrix.com

Lake City, Forell Elsseser Engineers, San Francisco, and members of the Utah State Capitol Preservation Committee in the selection of response spectra for use in design of the base isolation system.

SEISMIC SOURCE CHARACTERIZATION

To evaluate site-specific earthquake ground motions for this study, a probabilistic seismic hazard analysis (PSHA) was performed to estimate the relationship between the level of ground shaking and the probability that the level will be exceeded during specified time periods. The basic components of a PSHA are a seismic source model that characterizes potential sources of earthquakes in the site region and attenuation relationships that predict ground motion amplitudes at the site as a function of seismic source parameters and source-to-site distances. An important part of the current methodology for conducting a comprehensive site-specific PSHA is the explicit incorporation of uncertainty in characterizing the input parameters: location and geometry of seismic sources, maximum earthquake magnitudes, frequency of occurrence of potentially damaging earthquakes, and the characteristics of earthquake ground motion attenuation. This approach allows the resulting uncertainty in the analysis results to be quantified and the sensitivity to different modeling assumptions to be examined. A logic tree approach is used to incorporate credible alternatives for seismic source interpretations, seismic source parameters, and ground motion attenuation models (Figure 1).

Seismic sources include all structures that have some potential for causing strong ground shaking at the site. The seismic source model developed for this study includes two types of sources: (1) *fault-specific sources,* which include mapped late Quaternary faults, and (2) *seismic source zones* to account for seismicity that cannot be attributed to fault-specific sources included in the model.

Fault Sources

We evaluated potential active faults located within 50 km of the State Capitol site (Figure 2) that were judged to be capable of generating magnitude 5 or larger earthquakes and are inferred to have had multiple Holocene-late Pleistocene displacements. The key parameters used to define the seismic hazard potential of significant crustal fault seismic sources are: total fault length and plan view geometry; probability of activity; maximum magnitude; and recurrence parameters. The assessment of these parameters is based on consideration of the maximum rupture length of faults, seismogenic crustal thickness and downdip geometry (used to estimate downdip width), fault slip rates, and paleoearthquake event intervals, and timing of paleoearthquakes. Because the result of the hazard analyses (as described later in this paper) showed that the dominant contribution to hazard results from the Wasatch fault zone, we present a summary of the source characterization data only for the Wasatch fault zone in this paper. The source characterization for other active faults is included in the Geomatrix report (AMEC [1]).

Wasatch Fault Zone

The 370-km-long Wasatch fault zone forms the eastern boundary of the Basin and Range province (Figure 2), and is characterized by nine westward-dipping normal fault segments that exhibit late Pleistocene or younger activity (Machette [4]); Hecker [5]). Three of the central five segments of the Wasatch fault zone extend to within 30 km of the site: the Weber, Salt Lake City, and Provo segments. Paleoseismic studies show that there have been repeated large-magnitude (moment magnitude, **M** ~7 or larger) earthquakes during the Holocene along these segments of the Wasatch fault zone. A summary of the tectonic data for each of the nine segments is shown in Table 1. A summary of the geometry of the Salt Lake City segment, the closest to the Capitol site, is provided below.

The 46-km-long Salt Lake City segment of the Wasatch fault zone consists of three left-stepping surface traces that bound the western base of the Wasatch Range within Salt Lake City (Machette [4]). The northern trace comprises the Warm Springs fault, the central traces comprise the East Bench fault, and the southern traces comprise the Cottonwood section. Two traces of the Warm Springs fault are

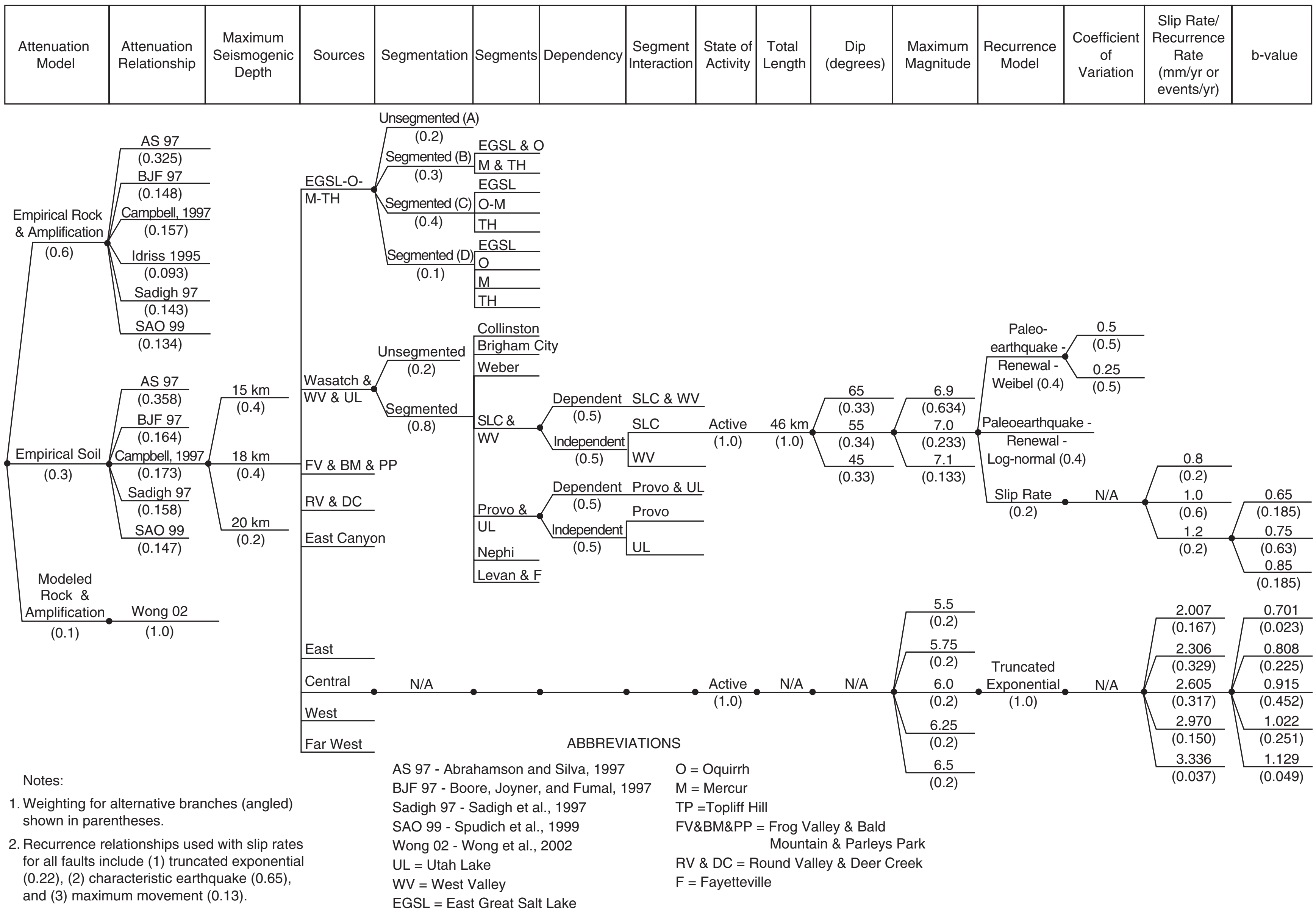

Figure 1. Seismic Hazard Logic Tree for PSHA

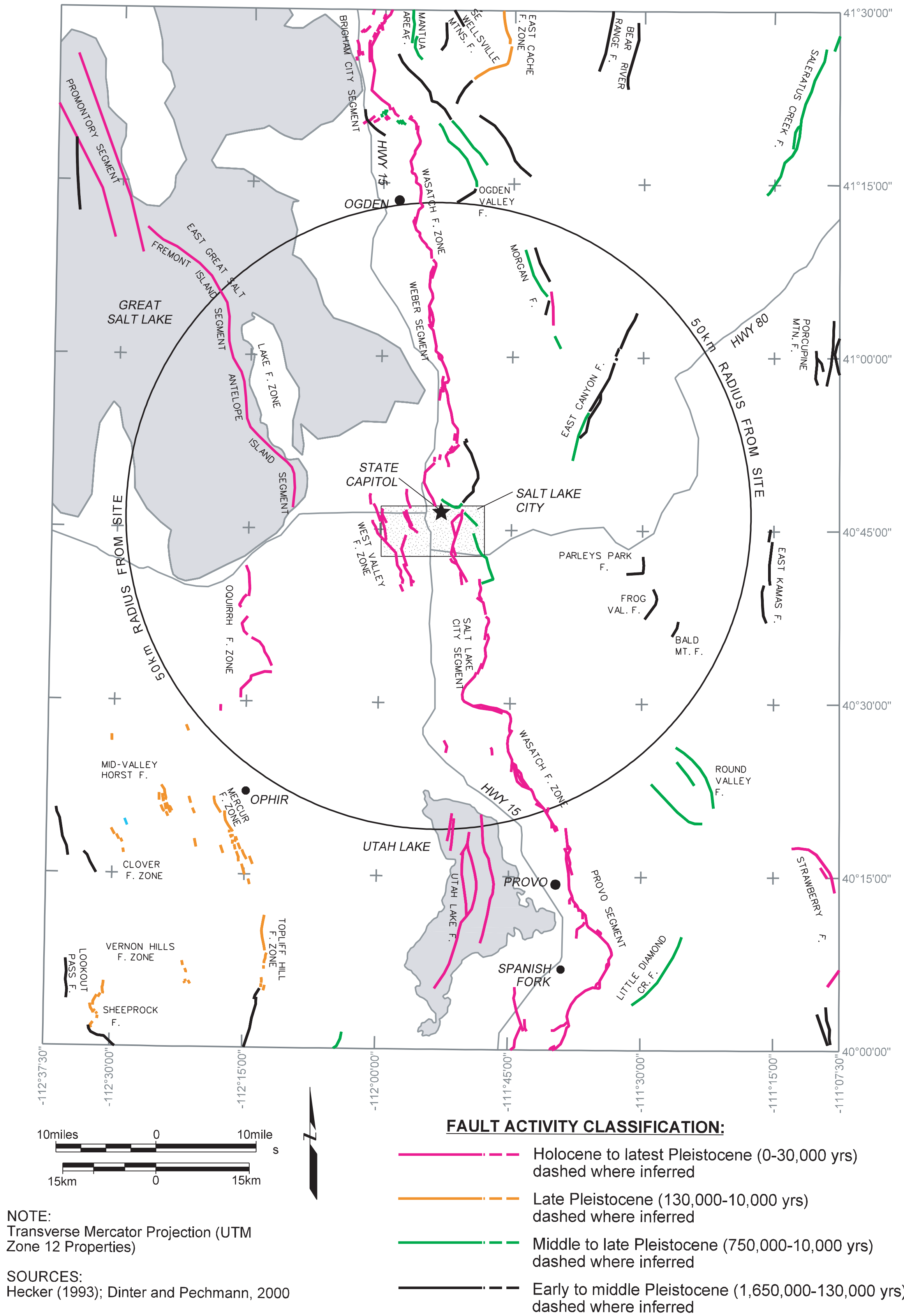

Figure 2. Map Showing Quaternary Faults in Site Region

inferred to extend southward from the range front into Salt Lake City, with the eastern-most trace lying about 0.3 km west of the State Capitol (AGRA [6]). This fault trace, which dips westward away from the site, is the closest approach of the Wasatch fault to the site.

Table 1. Tectonic Activity Information – Wasatch Fault Zone[2]

Segment	Age of Most Recent Movement (years)	Slip Rate (mm/yr) [Time Period, ka]	Recurrence Interval (years) [Time Period, ka]	Displacement Per Event (m)	Length (km)
Collinston	Late Pleistocene				30
Brigham City	3,600 2,125 ±104	0.75 [<4.7] 1.0 – 1.3 [<15]	1,100 – 3,600 [<4.7] 1,282 ±138	1.0 – 2.5	40
Weber	500? 1,000	1 – 3 [~6] 0.5 – 1.9 [<15]	1,300 [~6] 1,782 ±102	1 – 3	61
Salt Lake City	1,100 – 1,800 1,230 ±62	>1.0 [<8-9] 0.8 [<19]	4,000 [<8-9] 2,400 – 3,000 [<19] 1441 ±182	1.5 – 5.0?	46
Provo	500 – 650 618 ±30	1.1 – 1.3 [<5.3] 1.0 – 1.7 [<15]	2,400 [<5.3] 2,297 ±70	1.5 – 3	70
Nephi	300 or 500? 1,148 ±68	0.8 – 1.3? [<5.5?] 0.4 [70 to 4.3]	1,700 – 2,700? [<5.5?] 2,716 ±248	1.4 – 2.5	43
Levan	1,000?	<0.3 [<7.3]	>6,300 [<7.3]	1.8 –2.0	30

The west-dipping East Bench fault lies about 3 km east of the south end of the Warm Springs fault. We also consider an alternative rupture scenario where the East Bench fault extends northwestward in the subsurface to form a continuous fault with the Warm Spring fault. For this scenario, the State Capitol is considered to lie on the footwall block of the Wasatch fault. Alternatively, if the East Bench fault continues northward in the subsurface, it is possible that the northern extent of this fault may pass east of and beneath the site, such that the State Capitol could lie in the hanging wall of the East Bench fault. For this scenario, the closest approach of the East Bench fault is about 1.6 km. The 61-km-long Weber segment is about 5 km north of the State Capitol site at its closest approach, and the 69-km-long Provo segment is about 30 km south of the site at its closest approach.

Two rupture models for the Wasatch fault are considered: an unsegmented model and a segmented model. In the unsegmented model, the maximum rupture length is not constrained by the geologically defined segment boundaries and maximum rupture lengths up to 100 km are considered, allowing for the simultaneous rupture of adjacent segments (Youngs [7]). Based on the results of paleoseismic investigations, which suggest the segments have ruptured independently during past earthquakes (Youngs [7]; Machette, [4]), relatively low weight [0.2] is assigned to the unsegmented model compared to the segmented model [0.8]. Given the unsegmented model, the average slip rate is judged to be in the range of 0.5 to 3.0 mm/yr based on the range of values reported by Hecker [5] for the central five segments of the Wasatch fault (including the Brigham City, Weber, Salt Lake City, Provo, and Nephi segments). Given the segmented model, the maximum rupture length for each segment is taken as the total length of the geologically defined segments. The frequency of earthquakes is based on the recurrence data for past surface-faulting events compiled by McCalpin [8] for each of the segments.

[2] Data from Hecker [5], Black [29]; Lund [30]; Mattson [31]; McCalpin [8].

We use three alternative methods to estimate the recurrence of earthquakes on the five central segments of the Wasatch fault (Figures 1 and 2). We consider that the paleoseismic data for recurrence intervals, as summarized by McCalpin [8], provides the best estimate of the recurrence of large earthquakes. We assign 0.8 weight to estimates based on these data. As discussed by McCalpin [8], there are two approaches for using these data. The first is to make the standard assumption of a Poisson process and use the data to assess the average frequency of earthquakes. The second approach is to use so-called "real time" probabilistic models that assume a more periodic behavior for the occurrence of large earthquakes and use a renewal recurrence model to assess the probability of occurrence in the next t years, give that t_o years have elapsed since the last earthquake. We use two standard forms for the renewal model distribution presented in McCalpin [8], the Weibel distribution and the log-normal distribution, giving equal weight to each.

The critical parameter of the renewal model is the coefficient of variation (COV) of the recurrence intervals on an individual fault. We use two equally weighted estimates of 0.25 and 0.5 for the COV to compute probabilities of large (characteristic) earthquakes in the next fifty years for the five central segments. The smaller value is consistent with much of the late Holocene paleoseismic data from the Wasatch fault that indicates regular behavior, whereas the variation in late Pleistocene versus late Holocene recurrence for rupture of the Salt Lake City segment indicates that the fault behavior is not regular, favoring a higher COV, as noted by McCalpin [8, 9]. The recurrence rate for smaller earthquakes on the central five segments of the Wasatch fault is an exponential distribution (up to **M** 6.4) based on earthquakes occurring in a narrow zone along the Wasatch fault. The third alternative for recurrence estimation, weighted 0.2, uses the fault slip rates with the three recurrence models (truncated exponential, characteristic, and maximum moment) to estimate earthquake occurrence in the same manner as for the other faults.

Other Active Faults

Other Quaternary faults within 50 km of the site that are reported to have Holocene and/or Late Pleistocene displacement include the West Valley fault zone, Utah Lake fault zone, Topliff Hill fault, Mercur fault, Oquirrh fault, East Great Salt Lake fault zone, and several minor back valley faults located east of the Wasatch fault zone (Figures 1 and 2). Each of these faults was characterized and included in the source model as an independent seismic source, except that we assigned a weight of 0.5 to a model where the West Valley fault ruptures simultaneously with the Salt Lake City segment, and the Utah Lake fault ruptures simultaneously with the Provo segment of the Wasatch fault. The recurrence for each of these faults is based on available fault slip rate information, such as summarized by Hecker [5].

Regional Aerial Sources

Four areal source zones are incorporated into the seismic hazard model for this study, with the Wasatch fault zone forming the boundary between the central and eastern zones. These are shown as the East, Central, West, and Far West sources on the logic tree (Figure 1). We developed a catalog of independent earthquakes for the project region using available earthquake catalogs for the Intermountain Region. We analyzed the completeness of the catalog prepared for this study, and we used the maximum likelihood technique of Weichert [10] and the periods of complete catalog reporting to estimate the recurrence parameters for each of the seismic source zones. The uncertainty in the recurrence relationship for each source zone was modeled by specifying a range of possible b-values and seismicity rates and computing the relative likelihood that each of the resulting recurrence relationships generated the observed earthquake catalog. These relative likelihoods were normalized into discrete probability distributions for the recurrence parameters. We consider the maximum magnitude for an earthquake occurring in the seismic source zones to be uniformly distributed in the range of **M** 5.5 to 6.5, with a mean value of 6.0.

SITE GEOLOGIC SETTING

At the State Capitol site, which is located on the north side of Salt Lake City, mapped surficial deposits include upper Pleistocene lacustrine sand and gravel that ranges in thickness from a few feet to as much as 80 feet (Personius [11]). The surficial deposits overlie middle to lower Pleistocene lacustrine and alluvial deposits that extend to a depth of about 400 to 900 feet. The Pleistocene deposits directly overlie Tertiary conglomerate along the southern margin of the Salt Lake Salient (north of the Capitol) (Van Horn [12]), and these Tertiary rocks are inferred to underlie the Pleistocene deposits at the Capitol site.

Depth (feet)	Shear Wave Velocity (V_S, ft/sec)
0-23	730
23-43	1750
43-243	1930
243-833	3000
833-4770	6400

Based on the available geologic mapping, geotechnical borings, and geophysical measurements, including downhole, refraction microtremor (ReMi) and spectral analysis of surface waves (SASW) techniques, AMEC [1] recommended that the ReMi profile shown at the right be adopted to represent the shear wave velocity profile at the Capitol site. The average shear wave velocity for the upper 30 m (V_{S30}) of the ReMi profile (from 0 to 100 feet depth) is about 1380 feet per second (ft/sec). Based on the site classes listed in FEMA 356 (FEMA [2]) and the preferred shear wave velocity measurements for V_{S30}, the soils at the State Capitol site are classified as Site Class C, very dense soil and soft rock. The selection of the shear wave velocity profile was based on detailed analysis of multiple data sets (as listed above), some of which were characterized by much higher or much lower shear wave velocities, and corresponding to Site Class B or to Site Class D.

GROUND MOTION ATTENUATION MODELS

For this study, we utilize the results of the Yucca Mountain Ground Motion Expert Panel study (CRWMS M&O [13]) to modify California and Basin and Range region empirical ground motion relationships to the tectonic environment of the State Capitol site in Utah. These modifications account for the effects of the characteristics of the earthquake source and the crustal wave propagation path. Also following the Yucca Mountain Expert Panel approach, we adjust the selected attenuation relationships for the lower rate of ground motion attenuation (higher Q) in north-central Utah as compared to California.

Selected Empirical and Other Attenuation Relationships

Empirical attenuation relationships for firm soil conditions developed by Abrahamson [14], Boore [15], Campbell [16], Sadigh [17], and Spudich [18] are used in this study as the empirical firm soil attenuation group. Empirical relationships for soft rock site conditions by the previously listed authors and by Idriss [19], modified for the firm soil conditions at the State Capitol site (as described below), are used in this study as the empirical rock attenuation group. The relative weighting of each relationship as defined by the Yucca Mountain project team is shown on Figure 1.

Another recent study for the Salt Lake Valley region used both empirical attenuation relationships for soft rock site conditions and a numerical modeling approach (Wong [20]) to evaluate ground motion hazards. The numerical modeling approach used by Wong [20] is a point-source version of a stochastic ground motion model developed by Silva [21]. This stochastic attenuation model was utilized to compensate for the lack of region-specific attenuation relationships, and was developed for a soft rock site condition. We also use the Wong [20] stochastic attenuation relationship in this study, with modification for firm soil conditions as described below.

Region-Specific Soil Amplification Factors

Wong [20] developed a series of amplification factors for the various soil types and thickness ranges present in the Salt Lake Valley region to use with the empirical and stochastic attenuation relationships for soft rock conditions. We used the factors for the older alluvial fan/glacial gravel site response units for 400 to 800 feet thickness range. In addition, we represent the site factors as the average of the amplifications developed using the Electric Power Research Institute (EPRI [22]) and Peninsular Ranges modulus reduction curves (EPRI, [22]), and Silva [21], respectively). These soil amplification factors are applied to the empirical rock attenuation group, and to the rock attenuation relationship developed from the stochastic numerical ground motion modeling approach.

Attenuation Models for the PSHA

In summary, three groups/models for ground motion attenuation are included in the PSHA (with weights as shown on Figure 1): an empirical soil group; an empirical rock group with site amplification; and a numerical-modeled rock relationship with site amplification. The rock attenuation relationships with soil amplification are assigned larger weight in the logic tree because these relationships are considered to better represent the site conditions at the State Capitol site than the soil attenuation relationships.

A further modification of the ground motions is made to account for the fault interaction between the West Valley fault and Salt Lake City segment, and the Utah Lake fault zone and the Provo segment. In the situation where simultaneous rupture occurs on these fault pairs, the mean and standard deviation of the log amplitude of ground motion are increased by the average of the factors developed by the expert panel for the Yucca Mountain project (CRWMS M&O [13]) to account for interaction between simultaneous ruptures on parallel normal faults.

Comparison of Attenuation Relationships with Site Response Results

We calculated probabilistic and deterministic spectra, as described in the following section, both with and without the site amplification factors for comparison to the results of the site response studies carried out by AMEC [1] using the SHAKE computer program. We calculated amplification factors for three probabilities of exceedance (2%, 10%, and 50% in 50 years) and for a deterministic scenario earthquake for the empirical rock attenuation group (with amplification/without amplification) and we calculated amplification factors from a comparison of the empirical soil versus empirical rock attenuation relationships for the deterministic scenario earthquake. These amplification ratios are shown on Figure 3 along with the mean amplification ratios calculated from the results of the SHAKE site response analysis performed by AMEC [1]. The ratios plotted from the empirical and stochastic (modeled) attenuation relationships using the selected site amplification ratios are in good agreement with the ratios obtained using SHAKE. The maximum amplification of about 2 occurs at a period of about 1 second and decreases to a value of about 1.25 at periods equal to or greater than about 4 seconds. In contrast, the amplification based on the lower-weighted empirical soil attenuation relationships reaches a constant value of about 1.75 at periods equal to or greater than about 1.5 seconds.

PROBABILISTIC AND DETERMINISTIC SEISMIC HAZARD RESULTS, AND DEVELOPMENT OF HORIZONTAL AND VERTICAL RESPONSE SPECTRA

The results of the probabilistic seismic hazard analysis (PSHA) are presented as horizontal equal-probability-of-exceedance (i.e., equal-hazard) response spectra. Deterministic response spectra are developed for significant (controlling) seismic sources identified from the PSHA. These spectra are used to develop recommended design-level horizontal and vertical response spectra.

Probabilistic Seismic Hazard Results

For hazard computations, the fault-specific sources were modeled as segmented planar surfaces. The areal source zones were modeled as a set of closely spaced parallel fault planes occupying the source regions. The probability density function for distance to earthquake rupture for each source was computed assuming earthquake ruptures were uniformly distributed along the length of the fault plane. The depth distribution for earthquakes was based on the observed depth distribution for well-located earthquakes. The distance density functions were computed consistent with the distance measure used in each of the attenuation relationships. A rectangular rupture area for a given size earthquake is located at a random point on the fault plane for the distance calculations.

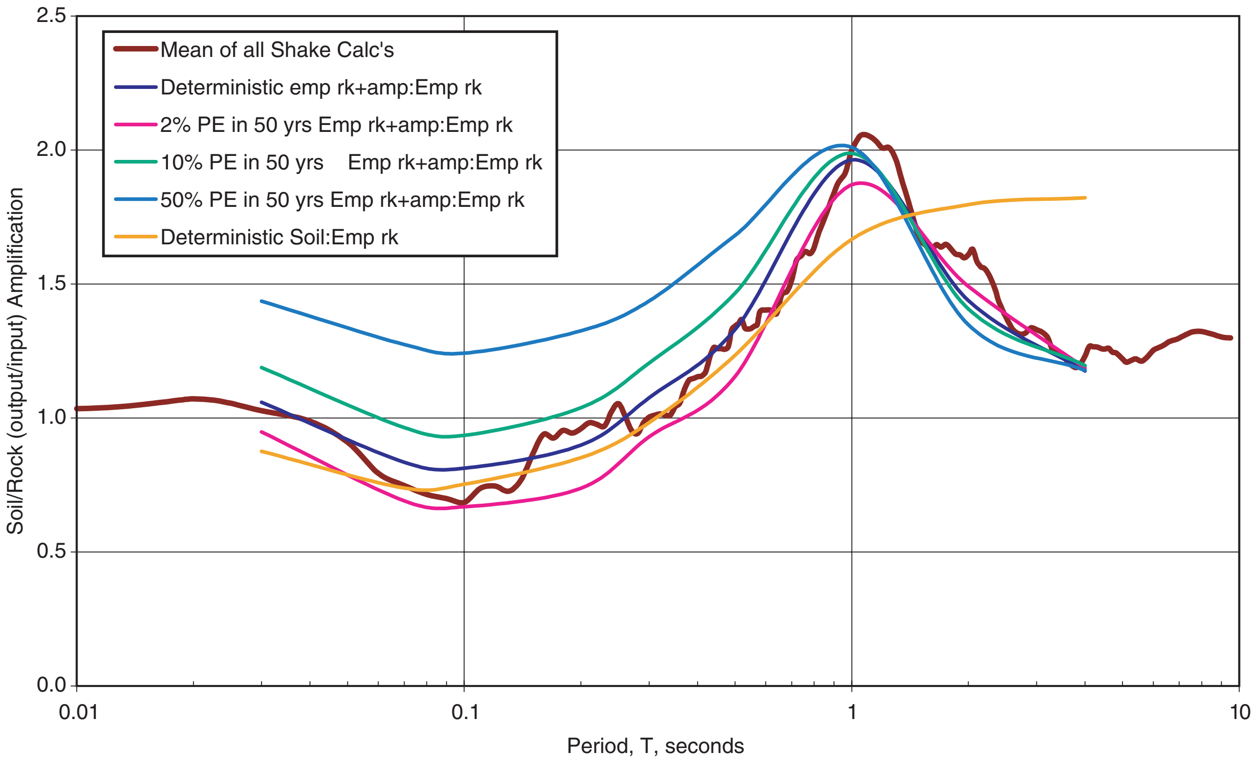

Figure 3. Comparison of Amplification Ratios from Wong [20] Amplification Factors and Rock Attenuation Relationships with Mean Soil-to-Rock Amplification from SHAKE Analysis

The rupture size of an event was specified by the relationship: ln (area [km^2]) = 2.095**M** – 7.88 developed from the results presented in Wells [23]. The specified relationship gives the mean rupture area for a specific magnitude rather than the median (mean log) rupture area. The hazard was computed with the distribution in peak ground motion about the median attenuation relationships truncated at three standard deviations.

Distributions for the annual frequency of exceeding various levels of peak ground acceleration (PGA) and spectral acceleration (SA) were developed by performing hazard computations with the input parameters defined by each branch of the logic tree. The hazard was computed considering the contributions of earthquakes of magnitude **M** 5 and larger. At each ground motion level, the complete set of results forms a discrete distribution for frequency of exceedance. The computed distributions were used to obtain the mean frequency of exceeding various levels of peak ground motion (mean hazard curve). The logic tree represents our best judgment as to the uncertainty in defining the input parameters.

The computed mean total hazard curves for horizontal PGA and for 5%-damped horizontal SA at a period of 1.0 second at the site, based on the empirical soil attenuation relationships, are shown on Figure 4. Also shown on Figure 4 are the mean hazard curves for the individual fault sources and the combined areal source zones. We note that the relative contributions to hazard from different seismic sources using the empirical soil attenuation relationships are representative of the relative contributions to hazard based on the empirical rock and modeled rock attenuation relationships. Figure 4 shows that as the level of ground motion increases with increasing return period, the Wasatch fault increasingly dominates the hazard at the site.

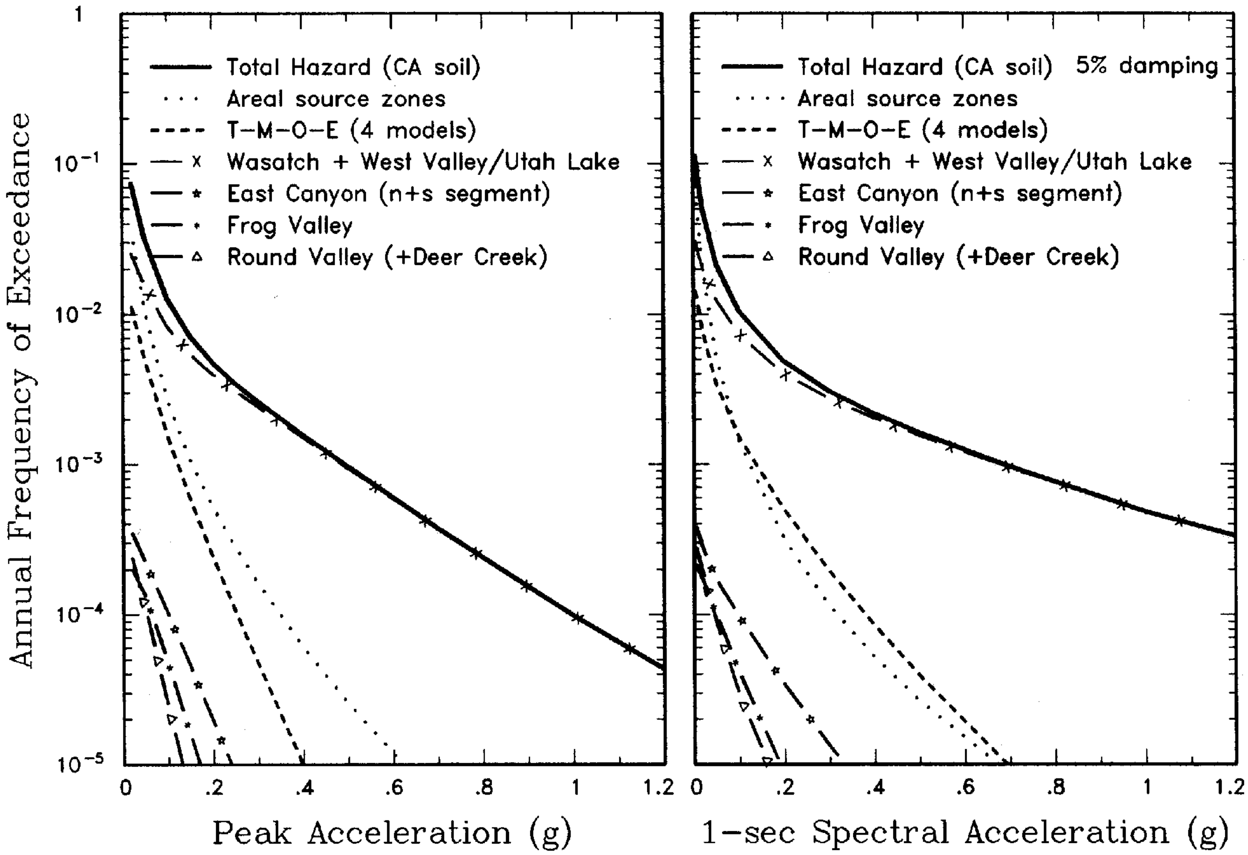

Figure 4. Contributions from Seismic Sources to Total Mean Hazard (Emp. Soil Attenuation) for Peak Ground Acceleration and 5%-Damped Spectral Acceleration at a Period of 1.0 Sec.

Magnitude and distance contributions to the total hazard for probabilities of exceedance of 10% in 50 years, corresponding to a return period of 475 years, are shown on Figure 5. The plots for the 475 year return period (and for the 2475 year return period) show that the dominant contribution to hazard results from earthquakes of **M** 6.75 to 7.25 occurring on the Salt Lake City and Weber segments of the Wasatch fault at distances of less than 10 km. For the 72 year return period, the contributions to hazard are broadly distributed from earthquakes of **M** 5.25 to 7.25, occurring at distances of 0 to 75 km.

Based on the above analyses and additional sensitivity analyses completed for the Geomatrix report (AMEC [1]), the major contributors to the uncertainty in the hazard are the selection of the alternative attenuation relationships, and assessment of maximum magnitude, recurrence rate and form of the magnitude distribution for the faults.

Development of Equal-Hazard Response Spectra

Probabilistic (equal-hazard) response spectra were developed from interpolation of the seismic hazard curves computed for PGA and 5%-damped SA at eight periods (0.07, 0.1, 0.2, 0.3, 0.5, 1.0, 2.0, and 4.0 seconds). The spectra represent the average horizontal component of ground motions incorporating the predictions of the ground motion attenuation relationships. The response spectra for the amplified empirical rock, amplified modeled rock, and soil attenuation groups were combined using the weighting shown on Figure 1 (weights of 0.6, 0.1, and 0.3, respectively) to develop mean equal-hazard response spectra. These results are 5%-damped equal-hazard horizontal response spectra for probabilities of exceedance of 50%, 10%, 5%, ~3.3%, ~2.5%, and 2% in 50 years, corresponding to return periods of 72, 475, 975, 1500, 2000, and 2475 years, respectively.

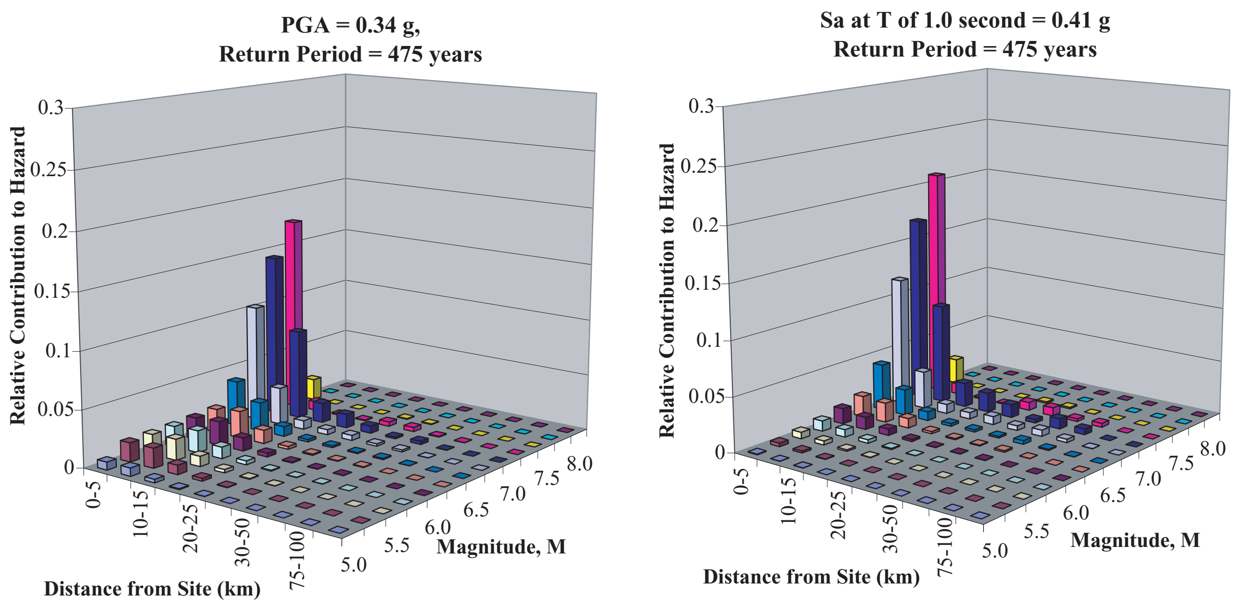

Note:
Magnitude contributions are binned by 0.25 units, centered
on quarter magnitude values (i.e. 6±0.125, 6.25±0.125)

Figure 5. Relative Contributions from Earthquakes in Different Magnitude and Distance Intervals to Hazard for Peak Ground Acceleration and 5% Damped Response Spectral Acceleration at a Period of 1.0 Second for 10% Probability of Exceedance in 50 Years

Development of Deterministic Response Spectra and BSE-1 and BSE-2 Response Spectra

Two levels of ground motions, Basic Safety Earthquake 1 (BSE-1) and BSE-2, were developed following the guidelines of FEMA 356 (FEMA, [2]). BSE-1 and BSE-2 ground motions are recommended for use in consideration of life safety and collapse prevention performance criteria, respectively. These spectra are developed from median probabilistic (2% and 10% probability of exceedance [PE] in 50 years), and median deterministic response spectra based on the characteristic earthquake for the controlling fault. The seismic hazard curves (Figure 4) and magnitude-distance contribution plot (Figure 5) for 2% and 10% PE in 50 years (and for 2% PE in 50 years) show that the controlling deterministic event is appropriately represented by a **M** 7.0 earthquake occurring on the Salt Lake City segment of the Wasatch fault at a distance of 0.3 km from the Capitol site.

Following FEMA 356, we select the lower of the spectral accelerations from the 2% PE in 50 years spectra and 1.5*median deterministic spectra to represent the BSE-2 spectrum (Figure 6). We found that these spectra are very similar (within about 2% to 7% of each other at all periods). The mean 10% PE in 50 years spectrum is selected as the BSE-1 spectrum (Figure 6) because it is always lower than 2/3*BSE-2 spectrum. Adjustment of these spectra for near-field fault effects is described in the following section

Modification of Equal-Hazard Response Spectra and BSE-1 and BSE-2 Response Spectra for Near-Field Fault Rupture Effects

The effects of rupture directivity and fault-normal/ fault-parallel motions on the ground motion hazard were incorporated using the model developed by Somerville [24]. The State Capitol site is located close to the Wasatch fault zone such that adjustment of the response spectra for both rupture directivity and fault normal-fault parallel effects need to be considered. We evaluated the contributions from earthquakes in different magnitude and distance ranges to the ground motion hazard at each probability level and for various ground motions (PGA, 1.0 second, and 4.0 second). Based on the dominant contribution of

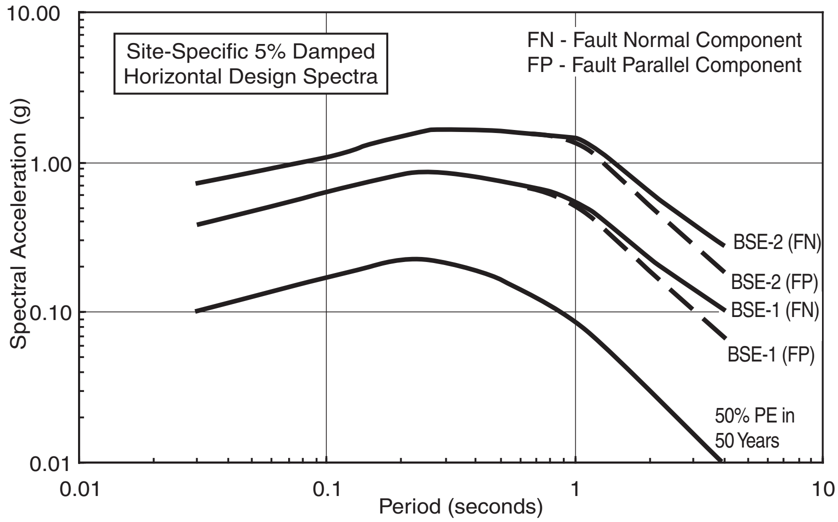

Figure 6. Horizontal Design Response Spectra for 50% Probability of Exceedance in 50 Years, BSE-1, and BSE-2.

characteristic earthquakes (~**M** 7) occurring at distances of less than 10 km on the Wasatch fault zone for the 10%, 5%, 3.3%, 2.5%, and 2% PE in 50 years levels, we judge that it is appropriate to adjust these spectra for near-field effects. At the higher probability level of 50% in 50 years, the ground motion hazard results from earthquakes having a wide range of magnitudes and distances (primarily earthquakes of less than **M** 6.75 at distances greater than 5 to 10 km). Because there is no single nearby controlling seismic source for the higher probability level, and because near-field effects do not appear to be significant at the mean magnitude and distance ranges of the contributing sources for the higher probability level (50% in 50 years), we judge that these response spectra do not need to be adjusted for near-field effects.

To estimate the near-field effects, it is necessary to characterize the geometry of the fault source/ earthquake rupture with respect to the site location. The Wasatch fault trends generally north-south, which represents the fault parallel direction. The fault normal direction is east-west. Because the Capitol site lies near a stepover region between the Warm Springs and East Bench faults, it is possible that the effective position of the Capitol site is either on the hanging wall or on the footwall with respect to potential near-field effects for rupture on the Wasatch fault. Therefore, we evaluated two potential geometries for the location of the Capitol site with respect to the Wasatch fault.

In one scenario, the Capitol site lies on the footwall, at a distance of 0.3 km from the surface trace of the Warm Springs fault (dipping 55° westward away from the Capitol site). In the second scenario, the Capitol site is located in the hanging wall at a distance of 1.6 km from the East Bench fault (dipping 55° westward under the Capitol site). We also considered two possible depths for rupture on the fault, the mean maximum depth of seismogenic rupture on the Wasatch fault (17.2 km) and a rupture at an intermediate depth on the fault plane (10 km). The mean fault dip (55°) from the seismic source characterization logic tree for the Wasatch fault (Figure 1) is used to construct the geometries used to evaluate values of Y and Φ for the directivity equations of Somerville [25]. We calculated mean directivity factors from the resulting four combinations of Y and Φ. We used equations with and without dependence on Φ (equally weighted) to evaluate fault normal and fault parallel factors. The directivity and fault normal/fault parallel factors were combined into a single period-dependent near-field factor that ranges from 1.0 at 0.5-second SA for both fault normal and fault parallel components to 1.7 at 4.0-second SA for the fault normal component and to 1.1 at 4.0-second SA for the fault parallel component. The fault parallel component is based on the average horizontal component for directivity, without reduction for fault parallel factors of less than 1.0, because we are uncertain that a reduction in SA due to a fault parallel effect is appropriate. The resulting BSE-1 and BSE-2 fault normal and fault parallel components of ground motion are shown on Figure 6.

Additional Analyses
Additional analyses that were completed included comparison of the BSE-1 and BSE-2 with the General Response Spectra of FEMA 356, assessment of factors for higher damping ratios, and development of vertical response spectra. We developed General Response Spectra for BSE-2 and BSE-1 following the general procedure in FEMA 356 to compare to the site-specific BSE-2 and BSE-1 spectra described above. Specifically, FEMA 356 indicates that the design spectra should not be less than 70% of the corresponding General Response Spectra (GRS). Comparison of the site-specific BSE-2 spectra modified for near-field effects with the 70% level of the GRS for BSE-2 indicates that the site-specific BSE-2 spectra are higher than the 70% level GRS spectra, except at short periods (~0.1 sec.). The site-specific short period SA therefore could be increased to the 70% level of the corresponding GRS, if these periods are significant for structural analyses. Comparison of the site-specific BSE-1 spectra modified for near-field effects with the 70% level of the GRS for 10% PE in 50 Years (BSE-1) indicates that the site specific BSE-1 spectrum is always higher than the 70% level GRS for BSE-1. Therefore no adjustment for BSE-1 was recommended.

We developed period-dependent factors for use in modifying the 5%-damped spectra to higher damping ratios of 10% and 20%. The factors are based on consideration of theoretical (Rosenblueth [25]) and empirical relationships (Abrahamson [26]; Idriss [19]) as described in Risk Engineering [27], as well as previous studies of the effects of damping on response spectra by Geomatrix.

To develop vertical response spectra, we evaluated ratios of vertical to horizontal ground motions estimated for the deterministic earthquake scenario described above and using vertical and horizontal ground motion attenuation relationships of Abrahamson [14], Campbell [16], and Campbell [28]. We considered ratios based on attenuation relationships for stiff soil (firm soil and very firm soil) and soft rock at the median and 84th percentile levels, with adjustments for normal faulting as recommended by the authors. The final ratios selected for use in the analysis are the average of the ratios for 84th percentile ground motions for stiff soil (firm soil) attenuation relationships of Abrahamson [14] and Campbell [29]. These ratios were developed for PGA and SA at periods equal to or less than 0.5 second, which was the period range of interest for vertical ground motion response of the Capitol.

CONCLUSIONS

Elements of the analyses especially significant for development of the design-level ground motions, specifically in incorporating all types of data relevant for the analyses and fully characterizing the uncertainty in the ground motions include the following items:

1. Characterization of the site conditions from multiple geotechnical and geophysical data sets to assess the depth to hard rock and the shear wave velocity at the site;
2. Incorporation of fault slip rate, event interval, and real-time probabilities for rupture on the Wasatch fault, including assessment of the coefficient of variation for recurrence intervals;
3. Modification of ground motions to account for fault interaction during simultaneous rupture of the Salt Lake City segment and West Valley fault;
4. Selection and weighting of multiple soil and rock attenuation models, including empirical relationships and numerical modeling approaches;
5. Evaluation and selection of region-specific site amplification factors;
6. Assessment of near-field fault rupture effects on ground motions, including development of alternative rupture models incorporating variation in fault geometry, hypocentral depth, and location for initiation of rupture of the Wasatch fault; and

7. Evaluation of ratios of vertical to horizontal spectral accelerations based on empirical attenuation relationships for development of vertical response spectra.

REFERENCES

[1] AMEC Earth and Environmental. "Geotechnical and ground motion data for Utah State Capitol, Salt Lake City, Utah." Prepared for Utah Capitol Preservation Committee, December 2003. [Includes report prepared by Geomatrix Consultants, Inc., "Site-Specific Response Spectra of Earthquake Ground Motions, Utah State Capitol, May 2003"]

[2] Federal Emergency Management Agency (FEMA). "Prestandard and Commentary for the Seismic Rehabilitation of Buildings (FEMA 356)." Prepared by the American Society of Civil Engineers, Reston, Virginia, for the FEMA, Washington, D.C., 2000.

[3] Cooper/Roberts Team. "Utah State Capitol Planning & Historic Structures Report." Report prepared for the State of Utah Capitol Preservation Board, September 13, 2000. (URL: http://utahstatecapitol.utah.gov/restoration/restoration.html).

[4] Machette MN, Personius SF, Nelson AR, Schwartz DP, Lund WR. "The Wasatch fault zone, Utah-segmentation and history of Holocene earthquakes." Journal of Structural Geology, 1991; 13: 137-149.

[5] Hecker S. "Quaternary tectonics of Utah with emphasis on earthquake-hazard characterization." Utah Geological Survey Bulletin 127, 1993; 157 p, 2 plates.

[6] AGRA Earth and Environmental. "Geoseismic and geotechnical evaluation, existing Utah state capitol building, remodel/seismic study, Salt Lake City, Utah." Report prepared for State of Utah Division of Facilities Construction and Management, Salt Lake City. DFCM Project No. FX95045-S, AGRA Job No. 6-817-2052, June 13, 1996.

[7] Youngs RR, Swan FH III, Power MP, Schwartz DP, Green RK. "Analysis of earthquake ground shaking hazard along the Wasatch Front, Utah." Gori PL, Hays WW, Editors. Assessment of regional earthquake hazards and risk along the Wasatch Front, Utah, volume II: U.S. Geological Survey Open-File Report 87-585, 1987; M1-M110.

[8] McCalpin JP, Nishenko SP. "Holocene paleoseismicity, temporal clustering, and probabilities of future large (M>7) earthquakes on the Wasatch fault zone, Utah." Journal of Geophysical Research 2000; 101 (B3): 6233-6253

[9] McCalpin JP. "Post-Bonneville paleoearthquake chronology of the Salt Lake City segment, Wasatch fault zone, from the 1999 'megatrench' site." Paleoseismology of Utah, 10: Utah Geological Survey Miscellaneous Publication 02-7, 2002, 38 p.

[10] Weichert DH. "Estimation of the earthquake recurrence parameters for unequal observation periods for different magnitudes." Bulletin of the Seismological Society of America, 1980; 70: 1337-1346.

[11] Personius SF, Scott WE. "Surficial geologic map of the Salt Lake City segment and part of adjacent segments of the Wasatch fault zone, Davis, Salt Lake, and Utah Counties, Utah." U.S. Geological Survey Miscellaneous Investigations Series Map I-2106, scale 1:50,000, 1992.

[12] Van Horn R. "Geologic map of pre-Quaternary rocks of the Salt Lake City North quadrangle, Davis and Salt Lake Counties, Utah." U.S. Geological Survey Miscellaneous Investigations Series Map I-1330, scale 1:24,000, 1981.

[13] Civilian Radioactive Waste Management System Management and Operating Contractor (CRWMS M&O). "Probabilistic seismic hazard analyses for fault displacement and vibratory ground motion at Yucca Mountain, Nevada." U.S. Department of Energy DE-AC04-94AL85000. Prepared for the U.S. Geological Survey, February 23, 1998.

[14] Abrahamson NA, Silva WJ. "Empirical response spectral attenuation relations for shallow crustal earthquakes." Seismological Research Letters, 1997; 68(1): 94-127.

[15] Boore DM, Joyner WB, Fumal TE. "Equations for estimating horizontal response spectra and peak acceleration from western North American earthquakes; A summary of recent work." Seismological Research Letters, 1997; 68(1): 128-153.

[16] Campbell, KW. “Empirical near-source attenuation relationships for horizontal and vertical components of peak ground acceleration, peak ground velocity, and pseudo-absolute acceleration response spectra.” Seismological Research Letters, 1997; 68(1): 154-179.
[17] Sadigh K, Chang CY, Egan JA, Makdisi F, Youngs RR. “Attenuation relationships for shallow crustal earthquakes based on California strong motion data.” Seismological Research Letters, 1997; 68(1): 180-189.
[18] Spudich P, Joyner WB, Lindh AG, Boore DM, Margaris BM, Fletcher JB. “SEA99 - A revised ground motion prediction relation for use in extensional tectonic regimes.” Bulletin of the Seismological Society of America, 1999; 89(5): 1156-1170.
[19] Idriss IM. “Selection of earthquake ground motions at rock sites.” Report prepared for the structures division, building and fire research laboratory. National Institute of Standards and Technology, Department of Civil Engineering, Univ. of California, Davis, March 1993 (revised from Sept. 1991).
[20] Wong I, Silva W, Olig S, Thomas P, Wright D, Ashland F, Gregor N, Pechmann J, Dober M, Christenson G, Gerth R. “Earthquake scenario and probabilistic ground shaking maps for the Salt Lake City, Utah, metropolitan area.” Utah Geological Survey Miscellaneous Publication MP-02-5 2002; 50 p.
[21]Silva WJ, Abrahamson NA, Toro G, Costantino C. “Description and validation of the stochastic ground motion model.” Unpublished report prepared for Brookhaven National Laboratory, 1997.
[22] Electric Power Research Institute (EPRI). “Guidelines for determining design basis ground motions.” EPRI TR-102293, 1993; 1-5.
[23] Wells DL, Coppersmith KJ. “New empirical relationships among magnitude, rupture length, rupture width, rupture area, and surface displacement.” Bulletin of the Seismological Society of America, 1994; 84: 974-1002.
[24] Somerville PG, Smith NF, Graves RW. “Modification of empirical strong ground motion attenuation relations to include the amplitude and duration effects of rupture directivity.” Seismological Research Letters, 1997; 68(1): 199-222.
[25] Rosenblueth E. “Characteristics of earthquakes.” Rosenblueth E, Editor. Design of Earthquake Resistant Structures, Chapter 1. New York: Wiley, 1980.
[26] Abrahamson NA, Silva WJ. “Empirical ground motion models.” Report submitted to Brookhaven National Laboratory, May 6, 1996.
[27] Risk Engineering, Inc. “Technical basis for revision of regulatory guidance on design ground motions: hazard- and risk-consistent ground motion spectra guidelines.” Prepared for U.S. Nuclear Regulatory Commission, Office of Nuclear Regulatory Research, Division of Engineering Technology, Washington, DC, 2001; NUREG/CR-6728.
[28] Campbell KW, Bozorgnia Y. “Updated near-source ground-motion (attenuation) relations for the horizontal and vertical components of peak ground acceleration and acceleration response spectra.” Bulletin of the Seismological Society of America, 2003; 93 (1): 314-331.
[29] Black BD, Lund WR, Schwartz DP, Gill HE, Mayes BH. “Paleoseismology of Utah, Volume 7; Paleoseismic investigation of the Salt Lake City segment of the Wasatch fault zone at the South Fork Dry Creek and Dry Gulch sites, Salt Lake County, Utah.” Utah Geological Survey Special Study 92, 1992, 22p.
[30] Lund WR, Black BD. “Paleoseismology of Utah, Volume 8 - Paleoseismic investigation at Rock Canyon, Provo segment, Wasatch fault zone, Utah County, Utah.” Utah Geological Survey Special Study 75, 1998; 41p.
[31] Mattson A, Bruhn RL. “Fault slip rates and initiation age based on diffusion equation modeling: Wasatch Fault Zone and eastern Great Basin.” Journal of Geophysical Research, 2001, 106(B7): 13,739-13,750.
[32] Dinter DA, Pechman, JC. “Paleoseismology of the East Great Salt Lake fault.” U.S. Geological Survey, NEHRP Summary Technical Report, Award No. 98HQGR1013, 2000, 6p. (http://erpweb.er.usgs.gov/reports/annsum/vol42/ni/G1013.pdf).